UPGRADE OF FERMILAB/NICADD PHOTOINJECTOR LABORATORY*

P. Piot, H. Edwards, Fermi National Accelerator Laboratory, Batavia, IL 60510, USA,
M. Hüning, Deutsches Elektronen-Synchrotron, Hamburg, D-22603 Germany,
J. Li, R. Tikhoplav, University of Rochester, Rochester, NY 14627, USA,
T. Koeth, Rutgers University, Piscataway, NJ 08854, USA.

Abstract

The Femilab/NICADD photoinjector laboratory is a 16 MeV electron accelerator dedicated to beam dynamics and advanced accelerator physics studies. FNPL will soon be capable of operating at ~ 40 MeV, after the installation of a high gradient TESLA cavity. In this paper we present the foreseen design for the upgraded facility along with its performance. We discuss the possibilities of using of FNPL as an injector for the superconducting module and test facility (SM&TF).

OVERVIEW OF THE NEW DESIGN

In collaboration with DESY we are planning to install a new TESLA-type superconducting cavity at the Fermilab/NICADD [1] photoinjector laboratory (FNPL) [1] downstream of the current existing TESLA cavity. The new cavity is expected to provide an average accelerating gradient $\bar{G}_{rf} \geq 25$ MV/m thereby boosting the beam energy above 40 MeV. This energy will open new possibilities for the experimental program [2]. In this paper we investigate a possible upgrade scenario where the new accelerator beamline is tailored to fit within the A0 building at Fermilab. The beamline (see Fig. 1) incorporates a user area for front-end experiments, and a drift space dedicated to the testing of either one of the two 3.9 GHz cavities developed at Fermilab [3]. Similarly to the present FNPL configuration, the beam is generated in an L-band ($f = 1.3$ GHz) rf-gun using a Cs_2Te photocathode impinged by a UV laser beam. The rf-gun cavity is surrounded by three solenoidal lenses. Upon exit from the rf-gun, the ∼4 MeV beam is accelerated by the two superconducting TESLA cavities (respectively operated at 12 MV/m and 25 MV/m).

After exiting the accelerating section, at $z \simeq 6$ m downstream of the photocathode, the beam transverse envelope can be controlled with a quadrupole doublet (D1) and a triplet (T1) located upstream of the magnetic bunch-compressor chicane. A skew quadrupole channel consisting of three quadrupoles is inserted between the doublet D1 and triplet T1 to produce flat beams [4, 5]. Downstream of the bunch compressor, a triplet (T2) follows to provide a control knob for the transverse beam envelope through possibly one of the 3.9 GHz cavities. After the 3.9 GHz cavity testing area, another triplet (T3) can be used to either (1) minimize the beam's betatron function at the screen located in the dispersive section downstream of the spectrometer or (2) to match the beam to desired Twiss parameters in the user area together with the downstream triplet (T4). The ~ 1.5 m-long user area located in the straight section downstream of the spectrometer dipole can also include focusing elements such as quadrupoles and solenoids depending on the experiment.

parameter	value(s)	units
laser temporal distrib.	Gaussian(s)	-
laser transverse distrib.	Uniform	-
laser rms duration	1.27, $\times 4$, $\times 8$	ps
laser rms trans. size	0.2-4	mm
beam charge	0.5 to 8	nC
initial kinetic energy	0.55	eV
rf-gun E-field on cathode	35	MV/m
peak E-field in cav 1	25	MV/m
peak E-field in cav 2	50	MV/m

Table 1: Nominal parameters for the various subsystems of the electron source and accelerating linac.

ROUND BEAM GENERATION

For the present calculation, we assume the laser time distribution to be Gaussian with pulse rms duration $\sigma_t = 1.3$ ps, as expected after frequency quadrupling of the infrared pulse of ∼6 ps FWHM [2]. Four or eight of this Gaussian pulses may be stacked via interferometric technique to produce a quasi uniform time distribution. The operation with one Gaussian pulse, and four or eight stacked Gaussian pulses is considered here. The profile of a laser consisting of n stacked pulse is $S(t) = \sum_{i=1}^{n} I_i \exp\left[-\frac{(x-\bar{x}_i)^2}{2\sigma_t^2}\right]$ where I_i is the intensity of each pulses, and $x_i = x_{i-1} + \delta t$ is the mean of each Gaussian distribution. The separation between the stacked Gaussian pulses δt are chosen to minimize the fluctuations of the density profile. A value of $\delta t = 1.6\sigma_t$ results in a 0.2% peak-to-peak intensity fluctuation. We assume I_i's are all equal and ignore possible interferences between adjacent pulses [3]. Using the beam parameters of Table 1 the trans-

* work supported by URA under contract No. DE-AC02-76CH00300 with US-DOE.

[1] NICADD is an acronym for Northern Illinois Center for Accelerator and Detector Development

[2] the laser parameters assumed are the ones expected after an upgrade of the IR oscillator using a new Time-Bandwidth oscillator

[3] In our pulse stacker design consecutive stacked pulses have orthogonal polarizations.

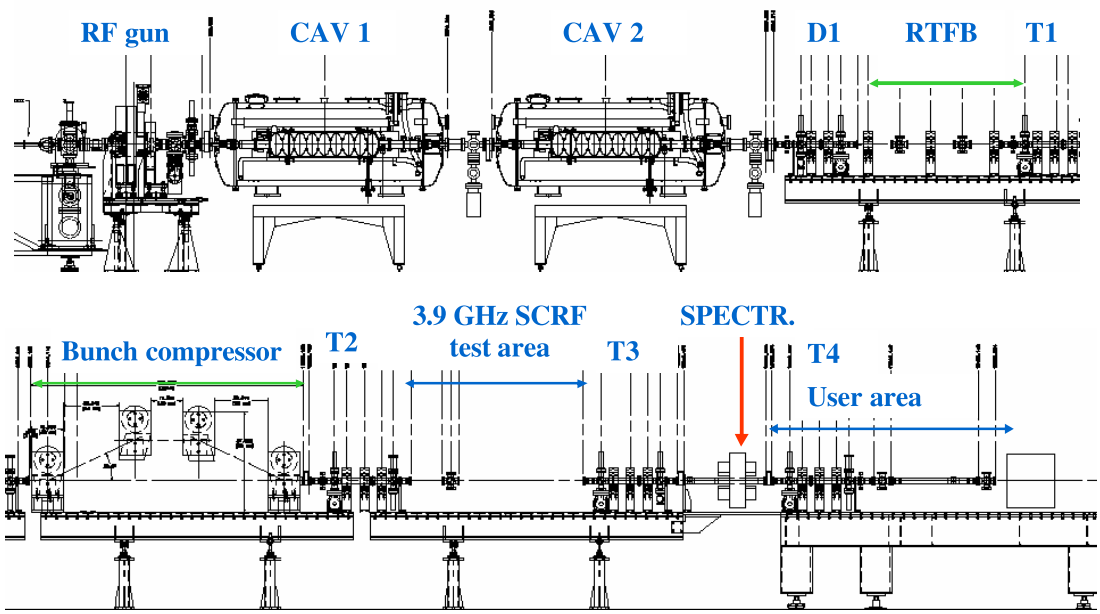

Figure 1: Overview of the FNPL upgrade beamline. The labels "CAV", "D", "T", stands respectively for SCRF cavity, doublet and triplet. The "3.9 GHz SCRF test" represents the region available in the beamline for testing either of the 3.9 GHz cavities being developed at Fermilab.

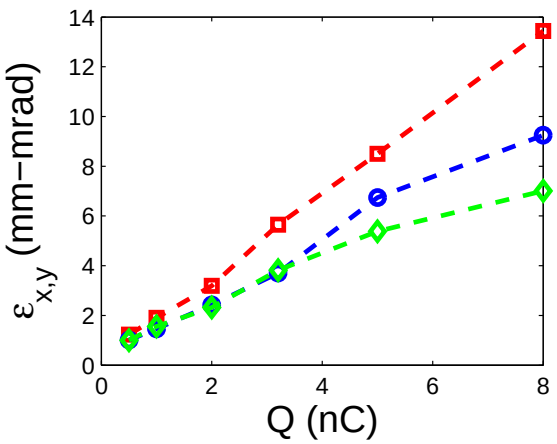

Figure 2: Optimized transverse emittance downstream of the accelerating sections versus charge for a photocathode laser consisting of one Gaussian pulse (red), four (blue) and eight (green) stacked Gaussian pulses.

verse emittance downstream of the accelerating section was optimized using the `sddsoptimize` [6] generic optimizer and the particle tracking program `astra` [7]. The variable for the optimization are the laser launch phase, the two solenoid profiles peak field and the laser transverse spot size. The optimized transverse emittances for various bunch charges and for the three cases of considered laser time distributions are shown in Fig. 2. The calculations support the use of longer laser pulse especially for high charges. For charges below 5 nC, simulations suggest that stacking four pulses should be sufficient, and the transverse emittance downstream of the accelerating section is frozen. This is an advantage of the 40 MeV beam compared to the present 16 MeV beam. The evolution of the transverse rms beam sizes along the transport line for $Q = 1$ nC is presented in Fig. 3: small spot sizes (70 μm) can be achieved in the user area despite the constraints imposed on the quadrupole strengths ($|k_1| < 50$ m^{-2}), and space charge effects are insignificant as inferred by comparing `synergia` tracking simulations with space charge algorithm on and off [8].

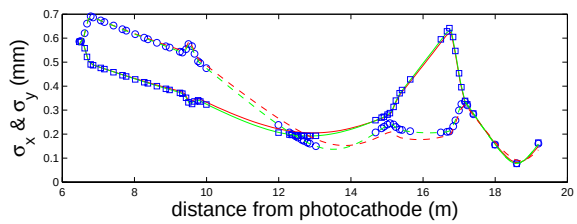

Figure 3: Transverse beam envelope σ_x (solid) and σ_y (dashed) evolutions along the transport line for a 1 nC bunch. The calculations are performed with `elegant` [9] (blue) and `synergia` space charge algorithm on (red) and off (green).

FLAT BEAM GENERATION

The production of flat beam is integrated in the present design: the beamline incorporates three skew quadrupoles whose strengths can be fitted to apply a net torque on the beam in order to remove its angular momentum. Angular-

momentum-dominated beams are produced by immersing the cathode in an axial magnetic field [11]. The round-to-flat beam transformer introduced in the upgraded beamline allows the generation of a flat beam with transverse emittance ratio $\sim$ 150 for bunch charge of 1 nC, while requiring moderate excitation strength ($|k_1| < 25$ m^{-2}) for the skew quadrupoles. An example of generated flat-beam emittances for a 1 nC beam is shown in Figure 4: the smaller of the flat-beam emittance is sensitive to chromatic effects and large fractional momentum spread $\sigma_\delta > 1$ % significantly degrades the flat beam emittance ratio.

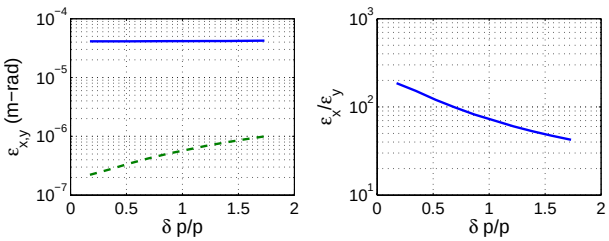

Figure 4: Example of transverse flat beam emittances (left) and corresponding emittance ratio (right) versus rms momentum spread. The bunch charge is 1 nC.

BUNCH COMPRESSION

At FNPL the bunch can be made shorter via magnetic compression scheme. The present bunch compressor chicane has a momentum compaction value $R_{56} \simeq -8$ cm, requiring an off-crest phase for maximum compression close to -35° to impart the required large correlated fractional momentum spread. Such a large momentum spread results in significant chromatic aberrations in the subsequent beamline. These aberrations have impacted the performance of some experiment (e.g. the density-transition plasma trapping experiment [12]) and prevent the compression of flat beam while maintaining a high emittance ratio [13].

The minimum bunch length occurs when the longitudinal phase space linear correlation satisfied the matching condition $d\delta/ds = -1/R_{56}$. The corresponding induced fractional momentum spread is approximately $\sigma_\delta \simeq \sigma_z/|R_{56}|$. For typical initial bunch length of 2.5 mm before compression, we have $\sigma_\delta \simeq 3\%$. Increasing $|R_{56}|$ would be beneficial in order to reduce the required fractional momentum spread and potential associated chromatic effects. On the other hand the momentum compaction of the chicane cannot be made arbitrarily large since the induced energy spread due to the bunch self-interaction via coherent synchrotron radiation scales with the radius of curvature ρ as $1/\rho^{2/3}$ ($\propto R_{56}^{1/3}$ for a given bunch compressor length). For a four-bend chicane with bending angle ψ, the bend length L_b and the drift length L_1 we have $R_{56} = 4L_b\left(\frac{1}{\cos\psi} - \frac{\psi}{\sin\psi}\right) + 2L_1\frac{\sin^2\psi}{\cos^3\psi}$. Due to space constraints we limit the maximum available projected length of the chicane to approximately 2.5 m and choose $L_1 = 0.5$ m, and $\psi = 30^\circ$ (using the current dipoles, we have $L_b = 0.3$ m). With these parameters we have $R_{56} = -26$ cm and maximum compression is obtained by operating CAV2 to -20° off-crest (CAV1 is kept on-crest). Such settings yield a rms correlated fractional momentum spread of approximately 1%. The dipoles and associated power supplies used at FNPL can be recycled with minor modifications. Detailed studies of the new bunch compressor including collective effects still remain to be done.

STATUS & PLANS

The booster cavity assembly (cavity and cryostat) used in the TTF-1 accelerator at DESY was decommissioned and shipped to Fermilab in November 2004. Work is ongoing to modify the cryostat and replace its cavity with a new high gradient cavity. We anticipate the energy upgrade of FNPL to occur in 2006. In the present report the design of the upgraded injector is bounded to fit in the A0 building. It is foreseen to move the FNPL in the MP9 building at Fermilab. The latter building is planned to host the superconducting module and test facility (SM&TF), a facility dedicated to R&D on superconducting linacs for ILC and the Fermilab proton-driver proposal [16]. FNPL could thus serve as an electron injector for the SM&TF and the ILC related R&D program. In parallel the electron beam produced at the SM&TF (eventually several 100's MeV) could be used for advanced accelerator physics R&D and beam physics studies.

REFERENCES

[1] informations available on-line at: `http://nicadd.niu.edu/fnpl`

[2] P. Piot, *et al.*, *Proc. of PAC 2005*, paper # TPAE037

[3] N. Solyak, *et al.*, *Proc. of LINAC 2004*, p. 797 (2004)

[4] R. Brinkmann, *et al.*, *Phys. Rev. ST Acc. Beams* **4**, 053501 (2004)

[5] D. Edwards, *et al.*, *Proc. of LINAC 2000*, p. 122 (2000)

[6] M. Borland and L. Emery, *Proc. 1995 ICALEPCS*, p. 653 (1996)

[7] K. Flöttmann *Astra user manual*

[8] J. Amundson and P. Spentzouris, *Proc. of PAC 2003*, p. 3195 (2003)

[9] M. Borland, ANL/APS report LS-287 (1999)

[10] J. Li, *et al.*, *Proc. of PAC 2005*, paper # WPAP043

[11] Y.-E Sun, *et al.*, *Phys. Rev. ST Acc. Beams* **7**, 123501 (2004)

[12] M. Thompson *et al.*, *Proc. of 11th AAC workshop*, AIP conf. Proc. **737**, p. 440 (2004)

[13] Y.-E Sun, *et al.*, *Proc. of LINAC 2004*, p. 150 (2004)

[14] K. Flöttmann , *et al.*, *Proc. of PAC 2001*, p. 2236 (2001)

[15] informations available on-line at: `http://ilc-dms.fnal.gov/Workgroups/SMTF/`

[16] G.W. Foster , *Proc. of PAC 2005*, paper # MOPB001